nature chemical engineering

Article

https://doi.org/10.1038/s44286-026-00389-w

High-titer, antibiotic-free, pilot-scale production of 1,3-propanediol by engineered *Corynebacterium*

Received: 8 June 2025

Accepted: 12 April 2026

Published online: 12 May 2026

Check for updates

Jae Sung Cho[1,2,6], Cindy Pricilia Surya Prabowo[1,2,6], Taehee Han[1,2], Cheon Woo Moon[1,2], Yoo-Sung Ko[1,2], Changhee Cho[3], Je Woong Kim[1,2], Won Jun Kim[4], Hyun Bae Bang[3], Jae Eun Lee[1,2], Minjung Ki[1,2], Namjin Jang[4] & Sang Yup Lee[1,2,5]

The microbial valorization of glycerol, a major biodiesel byproduct, into high-value chemicals remains challenging at industrially competitive titers. Here we engineered *Corynebacterium glutamicum* for high-level 1,3-propanediol (1,3-PDO) production, validating each step via fed-batch fermentation. First, *C. glutamicum* ATCC 13032 was metabolically engineered to produce 138 g l^{-1} 1,3-PDO from glucose–glycerol and 100.9 g l^{-1} from glycerol alone. Key engineering strategies included establishing glycerol uptake and 1,3-PDO biosynthetic pathways, minimizing byproducts and optimizing fed-batch fermentation. We then transferred these strategies to a newly isolated strain, *C. glutamicum* SC97. Further engineering, including antibiotic-free plasmid addiction system and *sucCD* overexpression, enabled 141.5 g l^{-1} 1,3-PDO at 2.95 g l^{-1} h^{-1} without antibiotics. Scalability was demonstrated at 30-l and 300-l pilot-scale fermentations, reaching 120.2 g l^{-1} and 127.8 g l^{-1} of 1,3-PDO, respectively. Techno-economic and life-cycle assessments support industrial feasibility and environmental impact, providing a robust blueprint for sustainable microbial 1,3-PDO production at scale.

Escalating concerns about climate change and depleting fossil resources have precipitated a substantial shift toward producing chemicals and materials from renewable, nonfood biomass[1]. A successful example is the commercialized production of biodiesel and biofuels through the transesterification of lipids from plant or animal oils[2–4]. However, this process produces a large amount of crude glycerol as a major by-product (100 kg glycerol per ton of biodiesel)[5], presenting a disposal challenge. Previously regarded as waste in the biodiesel industry, glycerol is now seen as having untapped potential as a substrate for the production of valuable chemicals[6–8]. One such chemical is 1,3-propanediol (1,3-PDO), a versatile organic compound essential in polymer manufacturing[9]. 1,3-PDO is largely used as a monomer for polytrimethylene terephthalate, in high-quality fibers for carpets, textiles and upholstery, and in polyurethanes for foams, adhesives and elastomers. Beyond polymers, 1,3-PDO is utilized in personal care products, certain food items, high-performance solvents and antifreeze

[1]Metabolic and Biomolecular Engineering National Research Laboratory and Systems Metabolic Engineering and Systems Healthcare Cross-Generation Collaborative Laboratory, Department of Chemical and Biomolecular Engineering (BK21 four), Korea Advanced Institute of Science and Technology, Daejeon, Republic of Korea. [2]BioProcess Engineering Research Center, Korea Advanced Institute of Science and Technology, Daejeon, Republic of Korea. [3]Bio Engineering Department, Hanwha Solutions R&D Institute, Daejeon, Republic of Korea. [4]Core Technology R&D Department, Hanwha Solutions R&D Institute, Daejeon, Republic of Korea. [5]Graduate School of Engineering Biology, Korea Advanced Institute of Science and Technology, Daejeon, Republic of Korea. [6]These authors contributed equally: Jae Sung Cho, Cindy Pricilia Surya Prabowo. e-mail: leesy@kaist.ac.kr

https://doi.org/10.1038/s44286-026-00389-w

agents, underscoring its wide-ranging industrial applications. Conventional production routes for 1,3-PDO involve acrolein hydration (Degussa–Dupont route), hydroformylation of ethylene oxide in the presence of phosphine (Shell route), or enzymatic transformation of glycerol[10]. The former two chemical methods are expensive and generate waste streams containing substances that cause pollution[11,12].

In industrial biotechnology, microorganisms serve as cell factories for converting nonfood biomass into valuable chemicals, materials, and fuels. Systems metabolic engineering has been pivotal in developing industrially competent strains capable of producing valuable chemicals[13]. Following the successful production of 1,3-PDO from glucose using metabolically engineered *Escherichia coli* by DuPont and Genencor, there have been increased efforts to microbially produce 1,3-PDO from renewable feedstocks[14,15] or directly from glycerol[16–18].

In nature, several species of microorganisms such as *Klebsiella*, *Clostridia*, *Enterobacter*, *Citrobacter* and *Lactobacilli* can convert glycerol to 1,3-PDO in two metabolic steps: the dehydration of glycerol to 3-hydroxypropionaldehyde (3-HPA) by glycerol dehydratase, followed by the reduction of 3-HPA to 1,3-PDO by 1,3-PDO dehydrogenase[19]. However, many isolated microorganisms capable of converting glycerol directly into 1,3-PDO pose challenges in genetic manipulation to produce desired chemicals, mainly due to the limited availability of genetic tools. Furthermore, most of these microorganisms capable of achieving high 1,3-PDO production levels (that is, *Klebsiella*, *Citrobacter* and *Enterobacter*) are classified in Hazard Group 2, complicating their use in industrial processes[16]. Meanwhile, Hazard Group 1 strains, such as *Lactobacillus*, produce 1,3-PDO with lower titers.

Corynebacterium glutamicum is a Gram-positive facultative anaerobe widely recognized for its industrial-scale fermentation capabilities, producing various products including amino acids[20,21]. With its long history as a fermentative microorganism in the food and feed industry, *C. glutamicum* has well-established fermentation processes, and recent advances in CRISPR–Cas-based genome engineering have further accelerated its metabolic engineering[20,22,23]. So far, there have been two reports of engineering *C. glutamicum* for 1,3-PDO production using various carbon sources at the laboratory scale[24,25]. In the first study, *C. glutamicum* ATCC 13032 was engineered to co-utilize glucose and glycerol, producing 14.4 g l^{-1} of 1,3-PDO with a yield of 0.89 mol mol^{-1} glycerol in a 500-ml shake flask, while simultaneously producing 32.5 g l^{-1} of L-glutamate as a byproduct[25]. More recently, advanced systems metabolic engineering enabled engineered *C. glutamicum* ATCC 13032 strains to produce 1,3-PDO with titers of 110.4 g l^{-1} 1,3-PDO from glucose (yield, 0.42 g g^{-1} glucose; productivity, 2.30 g l^{-1} h^{-1}) and 98.2 g l^{-1} 1,3-PDO from a glucose–xylose mixture (yield, 0.38 g g^{-1} (glucose and xylose); productivity, 2.04 g l^{-1} h^{-1}) in 5-l bioreactors, with byproduct formation remaining unresolved[24]. While these studies demonstrated the potential of *C. glutamicum* to produce 1,3-PDO, they were confined mostly to small-scale experiments using the well-characterized reference strain without exploring the challenges associated with pilot-scale production or prospective commercialization. This is a common limitation in metabolic engineering projects, where 5-l bioreactor experiments are typically used only as a final validation step for strains primarily optimized in shake flasks. As a result, critical factors such as strain robustness, scalability and process optimization are often overlooked during strain development. Addressing these limitations requires engineering strategies that not only bridge the gap between laboratory-scale successes and industrial feasibility but also extend to strains freshly isolated from the environment, enabling their adaptation to specific industrial processes.

Here, we describe the engineering strategies used to enable a wild-type *C. glutamicum* ATCC 13032 to produce high levels of 1,3-PDO and the adaptation of these strategies to a newly isolated *C. glutamicum* SC97 strain (Hanwha Solutions) for prospective commercialization (Fig. 1). Extensive metabolic engineering was performed on *C. glutamicum* ATCC 13032, incorporating fed-batch fermentation in

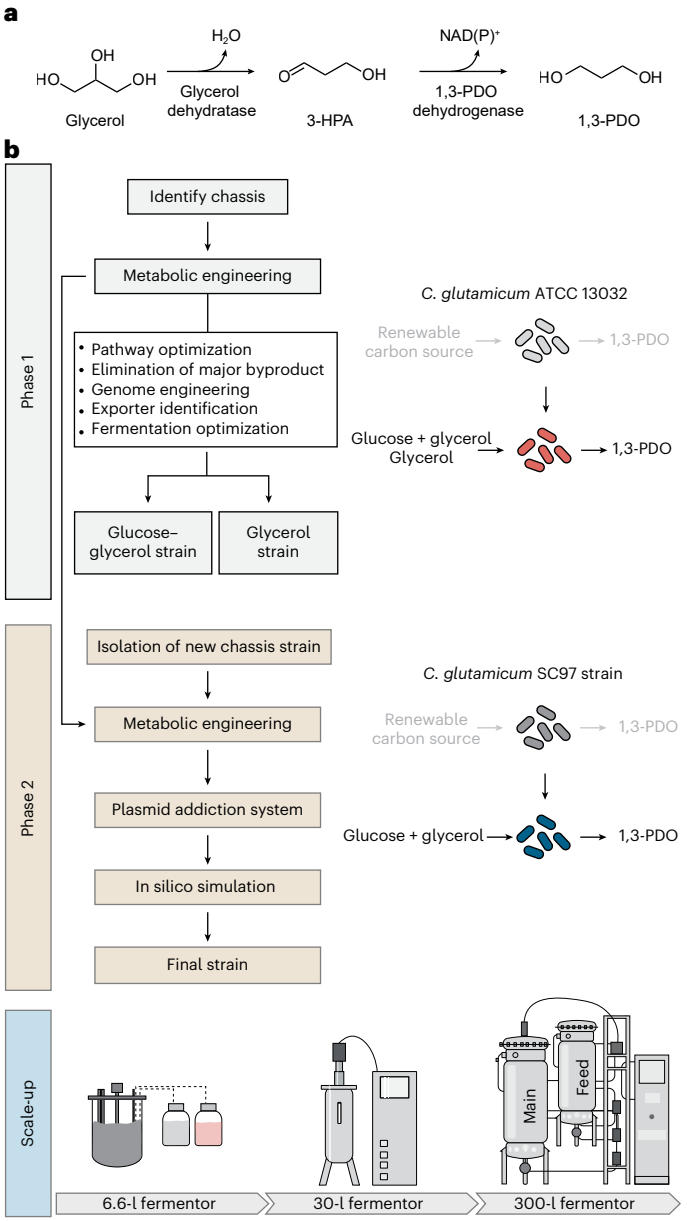

Fig. 1 | Summary of the 1,3-PDO strain development from wild-type *C. glutamicum* ATCC 13032 and its transition to the industrial strain *C. glutamicum* SC97. a, Biosynthetic conversion of glycerol to 1,3-PDO. **b**, Brief overview of the approach taken in this work.

6.6-l jar bioreactors at each step of strain development to establish an engineering blueprint for the *C. glutamicum* SC97 strain. Upon the initial assessment, the newly isolated strain achieved high-level 1,3-PDO production in fed-batch fermentation, comparable to that of the ATCC 13032-derived strain. To avoid antibiotic use in large-scale fermentations, which is economically and environmentally unfavorable, we used auxotrophy coupled with plasmid addiction systems to eliminate the need for antibiotic supplementation for plasmid maintenance. Further yield and productivity improvements were achieved through in silico simulations identifying gene targets for overexpression. A pilot-scale (30-l and 300-l) fermentation of the final engineered strain was performed to assess the feasibility of commercializing this biobased production of 1,3-PDO. Finally, techno-economic analysis (TEA) and life-cycle assessment (LCA) were performed to evaluate the economic competitiveness and sustainability of the overall production process.

Toxicity of 1,3-PDO to *C. glutamicum*

To assess whether *C. glutamicum* is a suitable host for high-level production of the non-native chemical 1,3-PDO, wild-type *C. glutamicum* ATCC 13032 was exposed to varying concentrations of 1,3-PDO (0, 25, 50, 75, 100 and 125 g l^{-1}). For comparison, two other hosts were included: *E. coli* W3110, which is well established for 1,3-PDO production, and *Klebsiella pneumoniae*, which can natively produce 1,3-PDO from glycerol. All three hosts demonstrated concentration-dependent growth inhibition by 1,3-PDO (Supplementary Fig. 1).

Shake-flask toxicity assays further revealed that, at 100 g l^{-1} 1,3-PDO, *C. glutamicum* retained ~84% of its final OD_{600} (optical density measured at 600 nm) relative to the 0 g l^{-1} control, whereas *E. coli* and *K. pneumoniae* retained only ~5.8% and ~62.9%, respectively (Supplementary Fig. 1a–c). Consistent with these end-point values, the specific growth rates at 100 g l^{-1} PDO were reduced by 2.87% (*C. glutamicum*), 53.53% (*E. coli*) and 8.73% (*K. pneumoniae*) of their respective controls at 0 g l^{-1} (Supplementary Fig. 1d). These results indicate that *C. glutamicum* is a robust strain with the potential to produce high titers of 1,3-PDO. Overall, it was determined that no further adaptive laboratory evolution was needed to increase *C. glutamicum*'s tolerance to 1,3-PDO before proceeding with further experiments.

Constructing a glycerol utilization pathway in *C. glutamicum*

C. glutamicum is unable to utilize glycerol for growth. Previous studies have demonstrated that *C. glutamicum* can metabolize glycerol for growth when *E. coli glpF*, *glpK* and *glpD* genes encoding aquaglyceroporin, glycerol kinase and glycerol 3-phosphate dehydrogenase, respectively, are introduced[26,27]. To construct a *C. glutamicum* capable of growth using glycerol as sole carbon source, plasmid pCS-glpFKD expressing *E. coli glpF*, *glpK* and *glpD* genes under synthetic promoter H36 was introduced to wild-type *C. glutamicum* ATCC 13032 strain (Supplementary Fig. 2a). The resulting strain WSG was able to grow with glycerol as sole carbon source in minimal media (Supplementary Fig. 2b), reaching an OD_{600} of 51.9, similar to that when glucose is used as sole carbon source (Supplementary Fig. 2c).

1,3-PDO biosynthesis from glycerol in *C. glutamicum*

Next, the 1,3-PDO biosynthetic pathway was constructed in *C. glutamicum*, in which glycerol is converted to 3-HPA by coenzyme B_{12}-dependent glycerol dehydratase. Two glycerol dehydratases and their reactivases in *Klebsiella pneumoniae*, encoded by the *pduCDEGH* and *dhaB*/*gdrAB* genes, were combined with three different alcohol dehydrogenases (*yqhD* from *E. coli*, *yqhD* from *K. pneumoniae* and *dhaT* from *K. pneumoniae*), six different plasmids pEK-dg-yE, pEK-dg-yK, pEK-dg-dK, pEK-pdu-yE, pEK-pdu-yK and pEK-pdu-dK were constructed (Supplementary Fig. 3a). *C. glutamicum* WSG strains harboring each plasmid were cultivated with glycerol as a sole carbon source. Flask cultivation results show that the configuration using *pduCDEGH* genes from *K. pneumoniae* and *yqhD* from *E. coli* produced the highest level of 1,3-PDO of 1.95 g l^{-1} (Supplementary Fig. 3b).

Fed-batch fermentation of the WSG strain harboring plasmid pEK-pdu-yE was performed to examine the production of 1,3-PDO using glycerol as a sole carbon source. Additional glycerol was fed when residual glycerol concentration approached 0 g l^{-1} during the fermentation. The WSG strain harboring plasmid pEK-pdu-yE produced 47.3 g l^{-1} of 1,3-PDO, with a productivity of 0.43 g l^{-1} h^{-1} and yield of 0.18 mol mol^{-1} (Supplementary Fig. 4, fermentation run 1). All yields presented in this study were calculated by dividing the total amount of 1,3-PDO produced by the total carbon sources utilized. Details regarding the production metrics, fermentation conditions and carbon sources used in each fermentation performed in this work are provided in Supplementary Table 1 and Supplementary Fermentation Dataset 1–30 (provide details on fermentation runs 1–30). Intriguingly, almost equal amounts of 3-hydroxypropionic acid (3-HP) were produced simultaneously with 1,3-PDO during the fermentation, reaching a maximum titer of 44.0 g l^{-1} of 3-HP. The overall engineering strategies implemented to enhance 1,3-PDO production, along with the representative fed-batch runs, are illustrated in Fig. 2.

Supplying reducing power through glucose addition

As glycerol metabolism bypasses the pentose phosphate (PP) pathway where *C. glutamicum* generates 70% of all NADPH[28], it was hypothesized that the limited NADPH required for the reductive conversion of 3-HPA to 1,3-PDO was supplied by regenerating NADPH from the oxidative conversion of 3-HPA to 3-HP by a native aldehyde dehydrogenase, thus forming a redox cycle (Supplementary Fig. 5).

To test this, glucose was added together with glycerol in varying ratios to observe its effect on 1,3-PDO and 3-HP production in shake-flask cultivation (Supplementary Fig. 6). The amount of 3-HP produced was inversely related to the amount of glucose supplied, with a 1:3 glucose-to-glycerol ratio producing the most 1,3-PDO and no 3-HP as a byproduct. The results here support that the 3-HP biosynthesis contributes to NADPH supply required for 1,3-PDO production under the glycerol-only condition. When glucose was added to meet the NADPH deficiency in the strain, an increase of 1,3-PDO production and a decrease of 3-HP accumulation was observed.

Fed-batch cultivation of WSG harboring pEK-pdu-yE with glucose and glycerol supplied at a 1:3 ratio successfully resulted in the production of 1,3-PDO at a high titer of 60.1 g l^{-1} and 3-HP largely reduced to 19.2 g l^{-1} (Supplementary Fig. 7, fermentation run 2). Further altering of the glucose ratio in the feed showed potential for enhancing 1,3-PDO production while reducing the byproduct 3-HP production; however, excessive increases, as observed in previous flask cultivations, did not improve yields (notably, a 1:1 ratio performed worse than 1:3 as shown in Supplementary Fig. 6). Adjusting the glucose-to-glycerol ratio to 1:2, the amount of 3-HP decreased to a titer of 5.99 g l^{-1}, and the production titer for 1,3-PDO reached a maximum titer of 82.2 g l^{-1} (Supplementary Fig. 8, fermentation run 3).

Aldehyde dehydrogenase screening for 3-HP in *C. glutamicum*

It was hypothesized that *C. glutamicum* possesses a native aldehyde dehydrogenase that converts 3-HPA to 3-HP to supply the NADPH demand (Fig. 3a and Supplementary Figs. 5 and 6a). Previous studies demonstrating 3-HP production in *C. glutamicum* have introduced heterologous genes into *C. glutamicum*[29,30]. At the time of manuscript preparation, a native enzyme responsible for the conversion of 3-HPA to 3-HP had not yet been identified. From the Kyoto Encyclopedia of Genes and Genomes (KEGG) database, 13 aldehyde dehydrogenases were selected, 7 of which were secondarily validated as aldehyde dehydrogenases using a deep-learning-based computational framework we had previously developed[31] by predicting their enzymatic classification from the corresponding protein sequences (Fig. 3b,c). All 13 potential candidates were subjected to rapid deletion in the wild-type *C. glutamicum* strain using previously developed CRISPR–Cas9 recombineering[32], where 11 strains, each with deletions of the potential aldehyde dehydrogenase, were successfully constructed (Supplementary Fig. 9). The individual deletion of *asd* (encoding aspartate-semialdehyde dehydrogenase) and *gapA* (encoding glyceraldehyde-3-phosphate dehydrogenase) were unsuccessful as these were essential genes in *C. glutamicum*. Plasmids pCS-glpFKD and pEK-pdu-yE were introduced to each of the 11 strains. Flask cultivation results demonstrated that aldehyde dehydrogenase Ald (encoded by *ald* gene) has high specificity toward 3-HP production in agreement with previous literature[24] and as indicated by the absence of 3-HP production (Fig. 3d). Before any further studies, the alcohol dehydrogenase gene *yqhD* was codon optimized for *C. glutamicum* to increase the flux toward 1,3-PDO production, which was shown to

https://doi.org/10.1038/s44286-026-00389-w

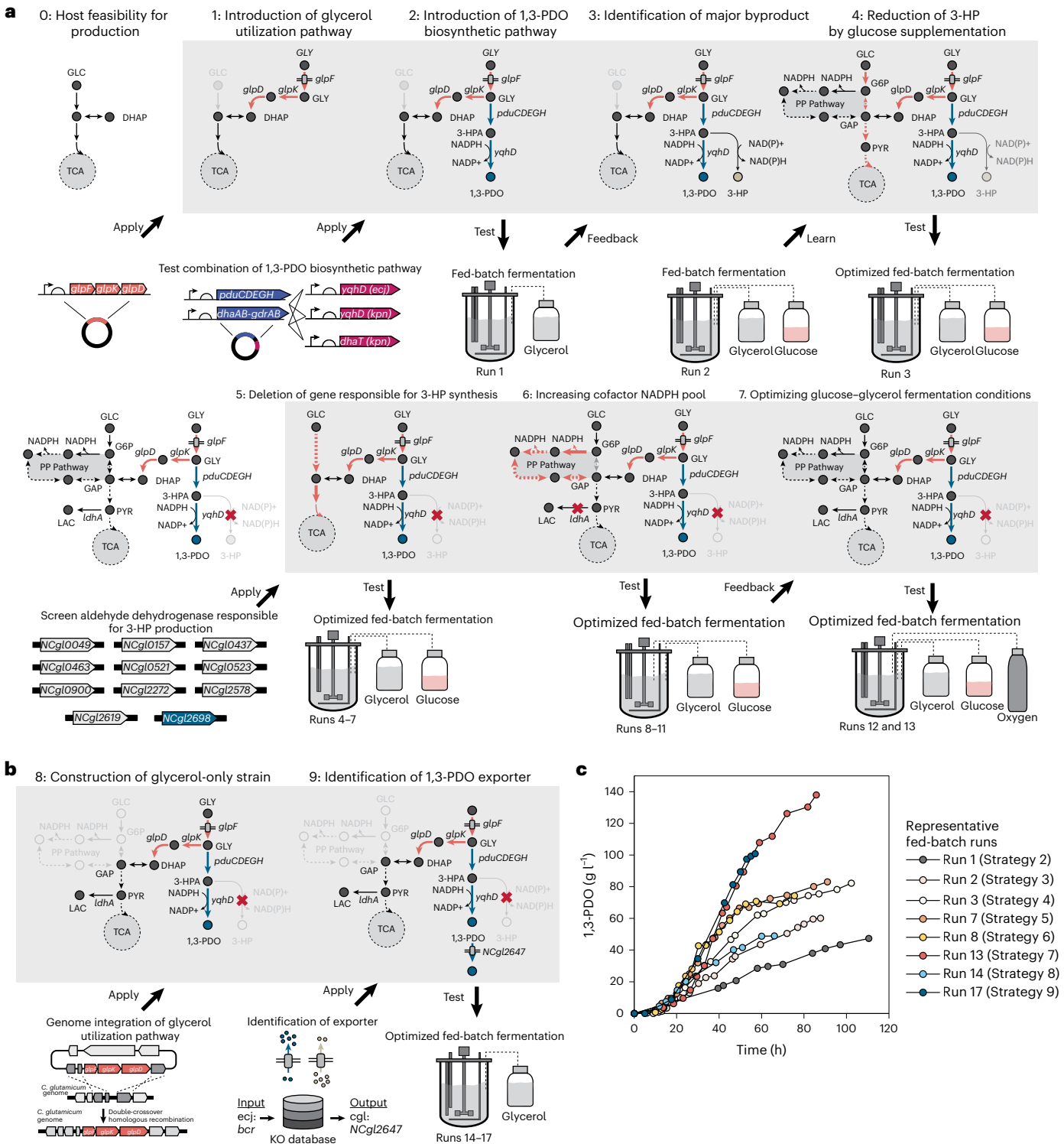

Fig. 2 | Overview of engineering strategies to optimize 1,3-PDO production in *C. glutamicum* ATCC 13032-derived strains. a, Engineering strategies applied to produce 1,3-PDO from glycerol and glucose, which include (0) initial assessment of the host strain for production via product tolerance testing, (1) construction and introduction of glycerol utilization pathway, (2) construction and optimization of 1,3-PDO biosynthetic pathway, (3) identification of 3-HP as a major byproduct of 1,3-PDO production, (4) supplementation of glucose to reduce byproduct 3-HP, (5) identification and deletion of gene responsible for byproduct 3-HP synthesis, (6) redox manipulation via PP pathway engineering and lactate reduction, and (7) optimization of fermentation conditions with the addition of oxygen. Note that all strategies undertaken were accompanied by performance assessment with fed-batch fermentations. **b**, Engineering strategies applied to produce 1,3-PDO from glycerol as sole carbon source, which include (8) genome-integration of glycerol-utilization pathway and adaptive-laboratory evolution, (9) identification of a 1,3-PDO exporter to enhance 1,3-PDO production. Abbreviations can be found in Supplementary Note 4. **c**, Representative fed-batch fermentation runs conducted illustrating 1,3-PDO production after each strategy implementation. Detailed fermentation conditions for each run can be found in the Supplementary Fermentation Dataset 1–30. ecj, *E. coli*; cgl, *C. glutamicum*.

https://doi.org/10.1038/s44286-026-00389-w

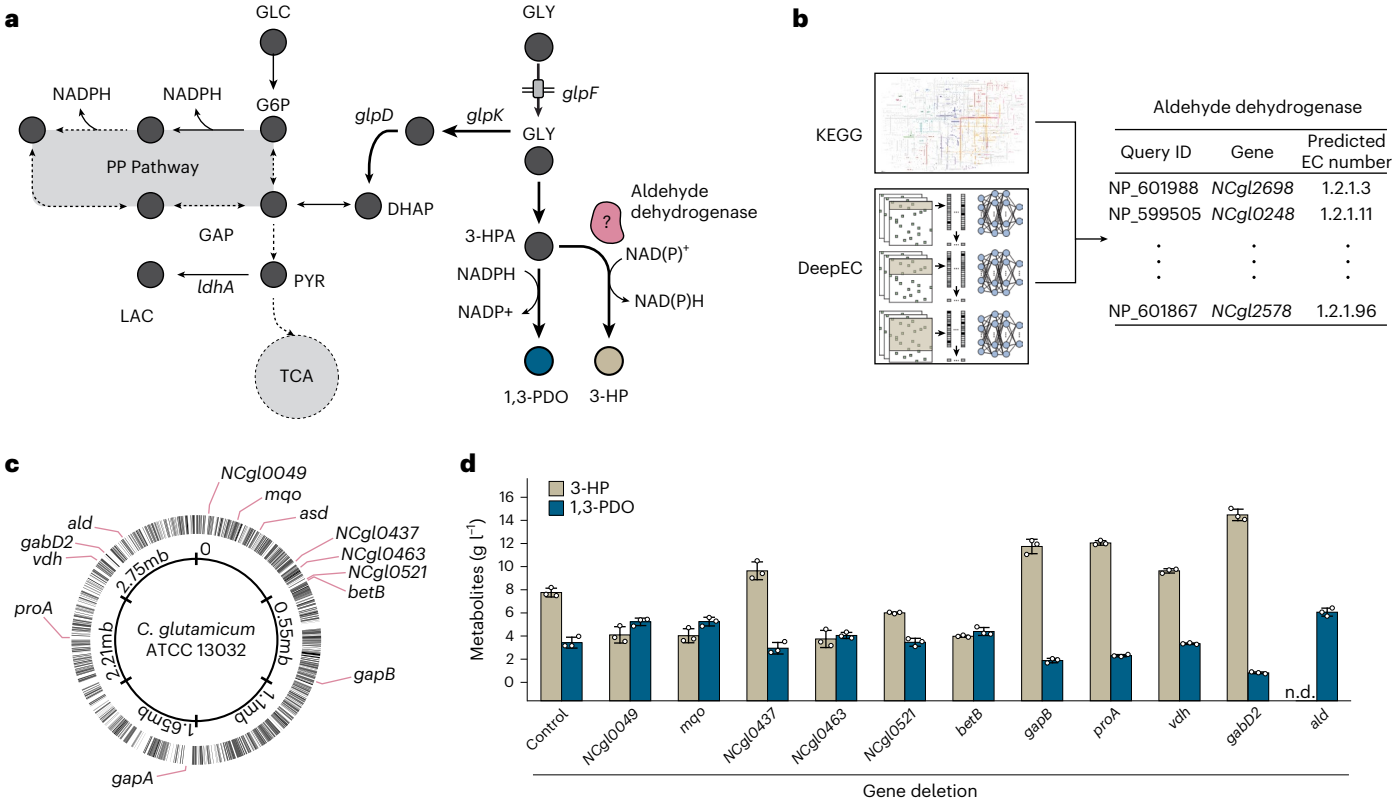

Fig. 3 | Screening of a native aldehyde dehydrogenase responsible for 3-HP formation. a, Metabolic map illustrating an unknown aldehyde dehydrogenase in competition with the 1,3-PDO synthetic pathway. **b**, Shortlisting of candidate gene targets using the KEGG database and secondary validation using DeepEC. **c**, Chromosomal location of the candidate aldehyde genes in the *C. glutamicum* genome. **d**, Effect of knockout of each candidate aldehyde dehydrogenase on the production of 1,3-PDO and 3-HP in *C. glutamicum*. All data are presented as mean ± s.d. of biological triplicates ($n = 3$). EC, Enzyme Commission; n.d., not detected.

have a positive effect (Supplementary Fig. 10). All future strains harbor the resulting plasmid pEK-pdu-yEco containing the codon-optimized *yqhD* gene. Fed-batch fermentation using glycerol as a sole carbon source with the *ald*-deleted *C. glutamicum* strain (designated WAH13) harboring pCS-glpFKD and pEK-pdu-yEco demonstrated a stagnation in growth (Supplementary Fig. 11, fermentation run 4). One evident reason is that the strain was now depleted of reducing power with the deletion of the aldehyde dehydrogenase *ald*. The subsequent addition of glucose and increase in air flow rate mitigated the reducing power deficiency arising from the *ald* deletion, thereby resulting in enhanced production of 1,3-PDO (83.03 g l^{-1}) when the air flow rate was set to 1 vvm (Supplementary Fig. 12, fermentation runs 5–7).

Redox engineering via PPP and lactate dehydrogenase deletion

To reduce the glucose uptake while increasing the NADPH pool, the *pgi* (encoding glucose-6-phosphate isomerase), *zwf* (encoding glucose-6-phosphate 1-dehydrogenase), *tkt* (encoding transketolase), *opcA* (encoding glucose-6-phosphate dehydrogenase), *pgl* (encoding 6-phosphogluconolactonase) and *tal* (encoding transaldolase) genes were manipulated to reroute the metabolic flux from glucose toward the PP pathway (Supplementary Fig. 13a), as this strategy has been demonstrated to have a positive effect on the production of L-ornithine and L-arginine in *C. glutamicum*[33,34]. To this end, the *C. glutamicum* strain W3PA (start codon of *pgi* manipulated from ATG to GTG and of *zwf* from GTG to ATG, and native promoter of *tkt* gene replaced with strong *sod* promoter) was constructed from strain WAH13. Fed-batch culture of this strain harboring pCS-glpFKD and pEK-pdu-yEco resulted in a lower titer of 74.2 g l^{-1} compared with strain WAH13 harboring the same plasmids. Also, a large amount of lactate, up to 12.9 g l^{-1}, was observed during the fermentation (Supplementary Fig. 13b, fermentation run 8). It was determined that the NADPH was not limiting, and the excess of NADPH had rather resulted in the production of lactate as a byproduct.

It was thus reasoned that the *ldhA* gene encoding lactate dehydrogenase should be deleted instead of enhancing the PP pathway as lactate might have been acting as a redox sink. The *ldhA* gene responsible for lactate production from pyruvate was deleted from strain WAH13 to construct strain WAL. Fed-batch fermentation of the WAL strain harboring plasmids pCS-glpFKD and pEK-pdu-yEco rather showed a reduction in carbon utilization rate and in 1,3-PDO production of 37.0 g l^{-1}, although no lactate had been produced (Supplementary Fig. 14, fermentation run 9). The results indicate that the deletion of *ldhA* is detrimental to the production of 1,3-PDO.

Optimizing glucose–glycerol fermentation conditions

All fed-batch fermentations were performed under microaerobic conditions up to this point, with constant agitation rate (600 rpm) without dissolved oxygen control. The fermentation process was then optimized using pH-stat feeding for glucose supplementation (Methods), which was found to not affect the 1,3-PDO production titer (Supplementary Fig. 15, fermentation runs 10 and 11). Given its operational simplicity, pH-stat feeding method was adopted for all subsequent fermentations requiring glucose.

In a particular run with the W3PA strain harboring plasmids pCS-glpFKD and pEK-pdu-yEco, lactate accumulation and reduced 1,3-PDO production was observed after 67.5 h (Supplementary Fig. 16, fermentation run 12). In light of this failed run, we transitioned to aerobic fermentation conditions by setting the dissolved oxygen levels to 10%, adjusting the agitation speed accordingly at 71 h to explore potential

outcomes before the planned termination of the run. To our surprise, this change led to a reduction in byproducts lactate and acetic acid and resumed the halted production of 1,3-PDO, reaching a final titer of 94.7 g l^{-1} (Supplementary Fig. 16, fermentation run 12). This outcome is consistent with the metabolic behavior of *C. glutamicum*, in which organic acids are formed predominantly under oxygen-limiting redox-overflow conditions[35]. It was determined that oxygen was a limiting factor to the production of 1,3-PDO. Consequently, the fermentation conditions were modified to ensure the dissolved oxygen would be maintained at 10%, regulating agitation speeds (600–1,000 rpm) and injecting pure oxygen once reaching maximum agitation speed. Under these conditions, the WAH13 strain harboring pCS-glpFKD and pEK-pdu-yEco reached a maximum titer of 138 g l^{-1} of 1,3-PDO with a yield of 0.50 mol mol^{-1} and productivity of 1.61 g l^{-1} h^{-1} (Supplementary Fig. 17, fermentation run 13). Taken together, the near-quantitative carbon flux toward 1,3-PDO, the absence of reduced overflow metabolites, and the close match between the observed yields and the redox-balanced stoichiometry of the engineered pathway indicate that the production phase proceeded under an effectively balanced intracellular redox state.

Integrating glycerol utilization pathway

Following the establishment of high-level 1,3-PDO production in *C. glutamicum*, we next engineered the strain to utilize glycerol as sole carbon source. To enable glycerol utilization, the *glpFKD* operon under the H36 promoter was introduced into the genome of the WAH13 strain (Supplementary Fig. 18a). The strain exhibited a long lag phase, with growth observed only after 72 h in shake flasks containing 40 g l^{-1} of glycerol as the sole carbon source (Supplementary Fig. 18b). The cells were adapted to glycerol over several passages (Supplementary Fig. 18c), and the adapted strain was introduced with plasmid pEK-pdu-yEco. Compared with the WAH13 harboring pEK-pdu-yEco, the resulting W13g strain produced a comparable level of 1,3-PDO when utilizing glucose and glycerol as carbon sources (Supplementary Fig. 19a) and effectively produced 4.2 g l^{-1} of 1,3-PDO with glycerol as the sole carbon source (Supplementary Fig. 19b) in flask cultivation. Sequencing of the glycerol utilization pathway region in the W13g strain revealed a promoter that emerged from adaptive mutations acquired during the adaptation process (Supplementary Fig. 20 and Supplementary Note 1).

Identification of a 1,3-PDO exporter

To further enhance the production of 1,3-PDO, potential exporters of 1,3-PDO were examined. A previous study indicated that the gene *bcr* from *E. coli* might encode for an active 1,3-PDO efflux pump, although it was not experimentally validated[36]. An ortholog of this enzyme, designated NCgl2647, was found to exist in *C. glutamicum* when analyzed through the KEGG Ortholog database (Supplementary Fig. 21a). A plasmid expressing *NCgl2647* under the strong H36 promoter (pCS-exp1) was introduced to W13g strain harboring pEK-pdu-yEco. Overexpression of the *NCgl2647* gene showed an increase of 30% of 1,3-PDO production in shake-flask cultivation (Supplementary Fig. 21b). In addition, a decrease in byproduct organic acid production was also observed (Supplementary Fig. 21c).

Optimizing fed-batch fermentation media and conditions

The W13g strain harboring plasmids pEK-pdu-yEco and pCS-exp1 was subject to further optimization of fed-batch fermentation conditions because the fermentation profiles are different when using glycerol as a sole carbon source. Yeast extract was replaced with corn steep liquor for all fermentations using the W13g strain for improved performance while ensuring low cost (Supplementary Note 2). Oxygen transfer was optimized for the W13g strain harboring pEK-pdu-yEco and pCS-exp1, and the condition for which the air flow rate was set at 1 vvm with the dissolved oxygen level controlled at 10% enabled 87.6 g l^{-1} of 1,3-PDO production (Supplementary Fig. 23, fermentation runs 14–16). Instead of manual feeding of glycerol whenever residual glycerol was low, the feeding strategy was changed to a pH-stat pulsed feeding strategy where glycerol was automatically fed when pH rose above 7.05. With the optimized fed-batch fermentation method, the final W13g strain harboring plasmids pEK-pdu-yEco and pCS-exp1 was capable of producing up to 100.9 g l^{-1} of 1,3-PDO with a yield of 0.21 mol mol^{-1} and productivity of 1.77 g l^{-1} h^{-1} (Supplementary Fig. 24, fermentation run 17). The representative 1,3-PDO fed-batch fermentation graphs are presented in Fig. 2c.

Transition to a newly isolated *C. glutamicum* SC97 strain

To this end, *C. glutamicum* ATCC 13032-derived strains successfully demonstrated high-level 1,3-PDO production: 138 g l^{-1} from glucose and glycerol, and 100.9 g l^{-1} from glycerol as the sole carbon source. Then, a newly isolated *C. glutamicum* SC97 strain (Hanwha Solutions) was engineered for the purpose of prospective commercialization of 1,3-PDO. At this stage of the work, in contrast to the development of the ATCC 13032-derived strain, which focused on utilizing glycerol as the primary carbon source, the SC97 strain development shifted toward utilizing a higher percentage of glucose driven by price fluctuations in carbon sources. Consequently, the glycerol utilization pathway was not introduced into this strain. Instead, glycerol was used as a substrate to be converted into 1,3-PDO.

To first assess the viability of the *C. glutamicum* SC97 strain for 1,3-PDO production, the *ald* gene, which is responsible for converting 3-HPA to 3-HP in *C. glutamicum*, was deleted in the SC97 strain to yield the PDO1 strain. Next, the 1,3-PDO biosynthetic pathway was introduced by transforming the PDO1 strain with plasmid pEK-pdu-yEco containing the *pduCDEGH* and $yqhD_{opt}$ genes. Plasmid pCS-exp1 harboring the *NCgl2647* gene encoding 1,3-PDO exporter, was introduced to the PDO1 strain harboring pEK-pdu-yEco. All flask cultures were carried out in the medium containing 40 g l^{-1} of glucose and 40 g l^{-1} of glycerol. The strain PDO1 (pEK-pdu-yEco and pCS-exp1) produced 7.9 g l^{-1} of 1,3-PDO in shake flasks, which is comparable to the titer achieved by the *C. glutamicum* ATCC 13032-derived WAH13 strain harboring the same plasmids (8 g l^{-1}) (Supplementary Fig. 25). To further examine the strain performance on a larger scale, fed-batch fermentation was carried out using the strain PDO1 harboring plasmids pEK-pdu-yEco and pCS-exp1. To our surprise, the strain PDO1 (pEK-pdu-yEco and pCS-exp1) produced a remarkable titer, reaching 143.9 g l^{-1} of 1,3-PDO (Supplementary Fig. 26, fermentation run 18). This result highlights the *C. glutamicum* SC97-based strain as a viable and highly promising host for industrial-scale 1,3-PDO production.

Screening of auxotroph/plasmid addiction systems

To further minimize production costs, we next sought to remove isopropyl β-D-1-thiogalactopyranoside (IPTG) and antibiotic selection altogether. First, we deleted the *lacI* gene from pEK-pdu-yEco to generate pPCO, thereby eliminating the need for IPTG induction. As the two-plasmid system (pPCO and pCS-exp1) would normally require two different antibiotics, we developed an auxotrophy-based plasmid addiction strategy, ensuring stable plasmid maintenance without antibiotic supplementation. Plasmid pPCO encodes the key enzymes for 1,3-PDO biosynthesis, while pCS-exp1 overexpresses *NCgl2647*, a newly identified 1,3-PDO exporter. Given the critical role of the plasmid pPCO in the 1,3-PDO pathway, auxotrophy screening was prioritized for this plasmid to ensure optimal expression of the biosynthetic genes. The maintenance of plasmid pCS-exp1 was fixed by using the β-alanine auxotrophy system, as it was previously demonstrated that overexpression of the *panD* gene, encoding aspartate decarboxylase, complemented β-alanine auxotrophy in *C. glutamicum*[37]. Therefore, for pCS-exp1 maintenance, a β-alanine auxotrophic strain was engineered by deleting

https://doi.org/10.1038/s44286-026-00389-w

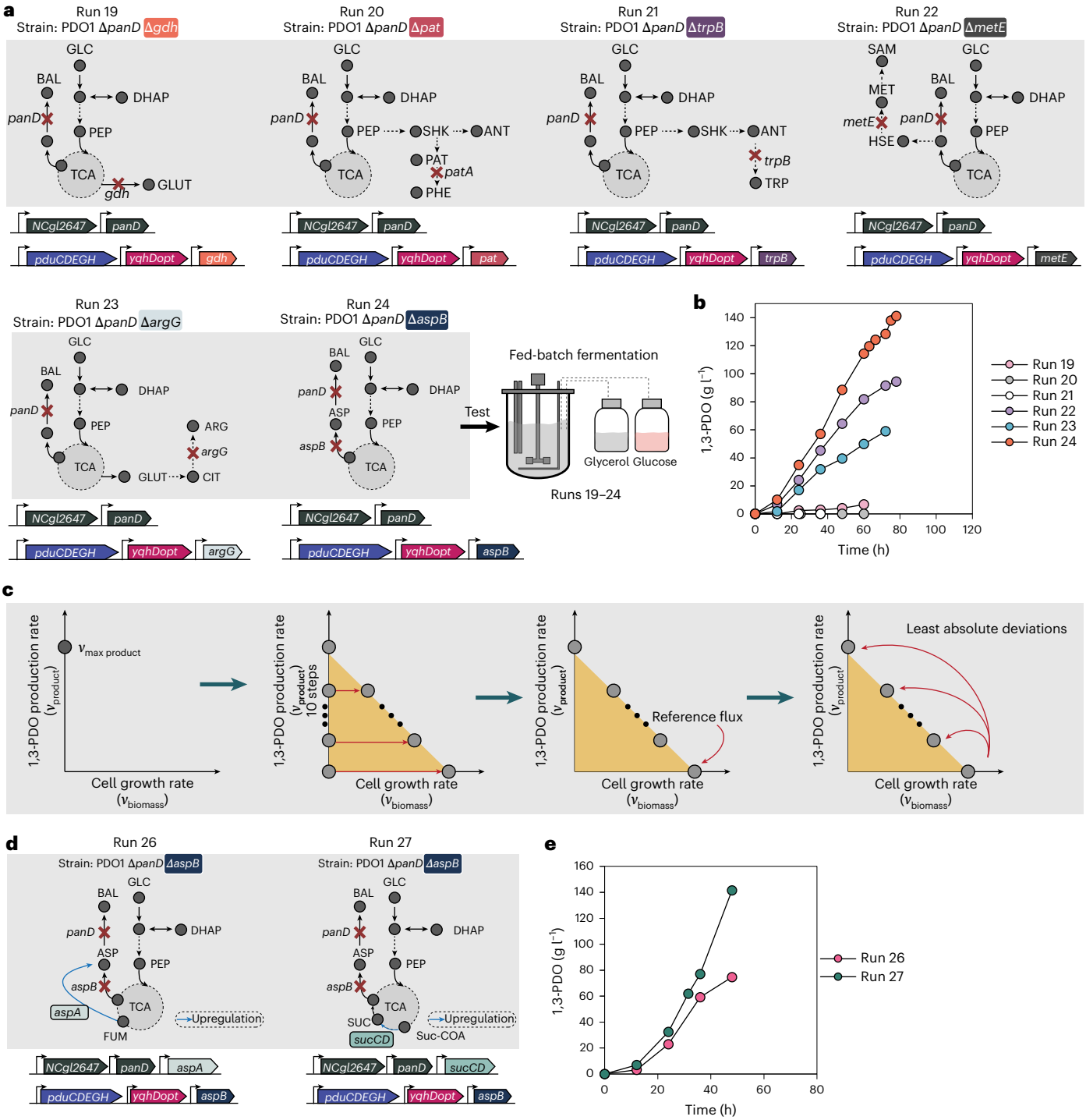

Fig. 4 | Overview of engineering strategies to optimize 1,3-PDO production in *C. glutamicum* SC97-derived strains. a, Metabolic pathway involved in the selected plasmid addiction/auxotroph systems. **b**, Representative fermentation runs of *C. glutamicum* SC97-derived strains with the plasmid addiction/auxotroph strategy used. **c**, Illustrative scheme of the in silico simulation prediction tool for yield improvement. v, rate (flux); $v_{product}$, product formation rate; $v_{biomass}$, biomass growth rate. **d**, Metabolic map of the pathway involving target overexpression genes resulting from in silico simulation predictions and their corresponding plasmid constructs. **e**, Representative fermentation runs harboring plasmids containing overexpression target genes resulting from in silico prediction.

the *panD* gene, yielding the PDO2 strain. Complementation of this auxotrophy was achieved by cloning *panD* under Its native promoter into pCS-exp1, resulting in the construction of plasmid pCS-exp1-panD.

Leveraging the strong and well-established amino acid pathways of *C. glutamicum*, we selected several key genes involved in amino acid biosynthesis to screen for an optimal auxotrophy/plasmid addiction system for maintaining the expression of the *pduCDEGH* and $yqhD_{opt}$ genes. Six complete pairs of double-auxotrophic strains were tested (Fig. 4a and Supplementary Table 2). Targeted single-gene deletion of the *gdh* (glutamate dehydrogenase), *pat* (phenylalanine aminotransferase), *trpB* (tryptophan synthase), *metE* (homocysteine methyltransferase), *argG* (arginosuccinate synthetase) and *aspB*

(aspartate aminotransferase) genes in the PDO2 strain resulted in the construction of the PDO2-1, PDO2-2, PDO2-3, PDO2-4, PDO2-5 and PDO2-6 strains, respectively. Then, to complement the auxotrophy, each corresponding gene was also cloned into pPCO under the H36 promoter, yielding plasmids pPCO-gdh, pPCO-pat, pPCO-trpB, pPCO-metE, pPCO-argG and pPCO-aspB. These plasmids were then cotransformed with pCS-exp1-panD into the respective auxotrophy strains. Next, fed-batch fermentations were performed on each of these transformed strains without antibiotic supplementation (Fig. 4b and Supplementary Figs. 27–32, fermentation runs 19–24). Among the six strains, the PDO2-6 strain harboring pPCO-aspB and pCS-exp1-panD exhibited the highest 1,3-PDO production with a titer of 141.1 g l^{-1} of 1,3-PDO with a yield and productivity of 0.47 mol mol^{-1} and 1.81 g l^{-1} h^{-1}, respectively (Supplementary Fig. 32, fermentation run 24). Strains with other pairs, except for *pat* and *trpB*, also demonstrated production of 1,3-PDO without antibiotic supplementation (Fig. 4). The robustness of the *aspB*/*panD* auxotrophy-based plasmid retention system was further validated through serial-transfer and quantitative polymerase chain reaction (qPCR)-based plasmid-stability analyses performed under complex-medium conditions, demonstrating stable maintenance of both plasmids over extended generational time scales (Supplementary Note 5, Supplementary Fig. 39 and Supplementary Tables 15 and 16).

In PDO2-6 harboring pPCO-aspB and pCS-exp1-panD, the *aspB* gene, which was responsible for converting oxaloacetate to L-aspartate, was deleted, resulting in the auxotrophy of L-aspartate. L-aspartate is a precursor of various amino acids, including L-lysine, L-isoleucine, L-threonine, L-methionine and β-alanine (Fig. 4a). Thus, there could have been a synergistic effect of both *aspB* and *panD* auxotrophy/plasmid addiction systems, as β-alanine production is dependent on the availability of L-aspartate. From this result, it was evident that amino acid auxotroph/plasmid addiction system is effective for developing an antibiotic-free strain, for high-level production of 1,3-PDO. The strategy was shown to maintain plasmids at the fed-batch fermentation-level, indicating the stability of the system.

An optimized sequence of the exporter *NCgl2647* gene was cloned to construct pCS-exp2-panD (Supplementary Note 3). In fed-batch fermentation, the PDO2-6 strain harboring plasmids pPCO-aspB and pCS-exp2-panD demonstrated improved production (148.2 g l^{-1}) and productivity (2.06 g l^{-1} h^{-1}) by 5% and 13.9%, respectively, while maintaining comparable yield (0.46 mol mol^{-1}) (Supplementary Fig. 33, fermentation run 25). Therefore, plasmid pCS-exp2-panD was used for all subsequent studies.

Genome-scale model-based gene engineering of *C. glutamicum* SC97

In industrial-scale fermentation, the yield and productivity are additional critical metrics for assessing the economical and marketing feasibility of the production process. Although a high-level 1,3-PDO titer of 148.2 g l^{-1} has been achieved, further improvements in yield and productivity remain necessary. To address this, in silico predictions were used to guide strain engineering strategies for optimizing 1,3-PDO production performance.

As the *C. glutamicum* SC97 strain was newly isolated in this study, next-generation sequencing was performed to obtain its genomic information. A genome-scale metabolic model of SC97 was constructed using CarveMe[38], which can be used for in silico simulations to identify gene targets for engineering. Initial efforts focused on increasing the NADPH pool and reducing growth, as these factors are correlated with 1,3-PDO yield. Statistical analysis identified five genes (Supplementary Table 3), with strong negative correlations between growth and NADPH availability as downregulation targets. These genes were downregulated by modifying their start codons (for example, ATG to GTG or GTG to TTG). However, flask cultivation of the resulting strains showed no substantial improvement in 1,3-PDO production, and in some cases, production was lower than that of the control strain (Supplementary Fig. 34).

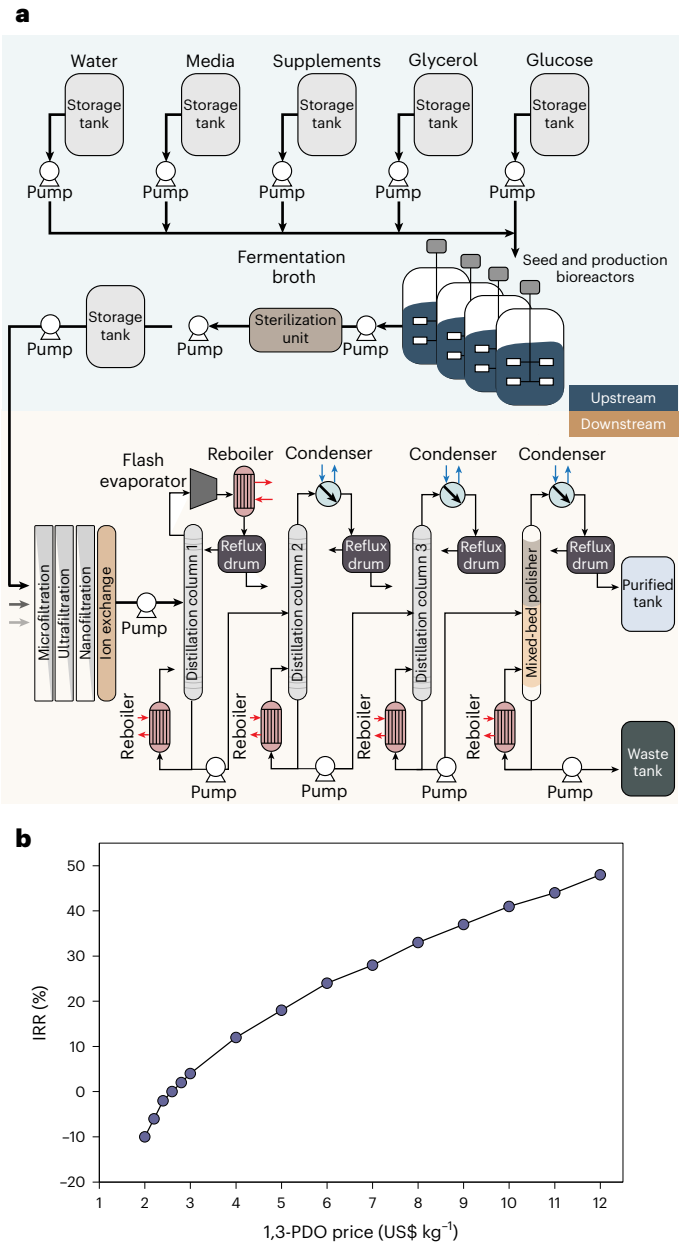

Fig. 5 | Overall scheme of the microbial-based 1,3-PDO production designed for TEA and LCA. a, Overall process configuration of the microbial 1,3-PDO production system used for TEA and LCA. This process configuration (cradle-to-gate boundary) was used for both economic and environmental evaluations. Aspen Plus (version 15, Aspen Technology) simulations provided mass balances, and cost estimation was carried out using APEA (Supplementary Note 6). **b**, Variation of internal rate of return (IRR) with 1,3-PDO selling price at a production scale of 5,600 metric tons per year, used to identify the economic break-even point. The base-case selling price was assumed to be US$4.00 kg^{-1}, and break-even occurs at approximately US$2.6 kg^{-1} (IRR ~0%).

Subsequent in silico analysis identified five overexpression target genes predicted to enhance 1,3-PDO production (Fig. 4c and Supplementary Table 3). These genes, linked to a positive linear relationship with 1,3-PDO production rates, were cloned individually into plasmid pCS-exp2-panD under the constitutive H36 promoter. Among the tested overexpression targets, overexpression of the *sucCD* gene (encodes for succinyl-CoA synthetase) and *aspA* gene (encodes for aspartate ammonia-lyase) led to substantial improvement in

https://doi.org/10.1038/s44286-026-00389-w

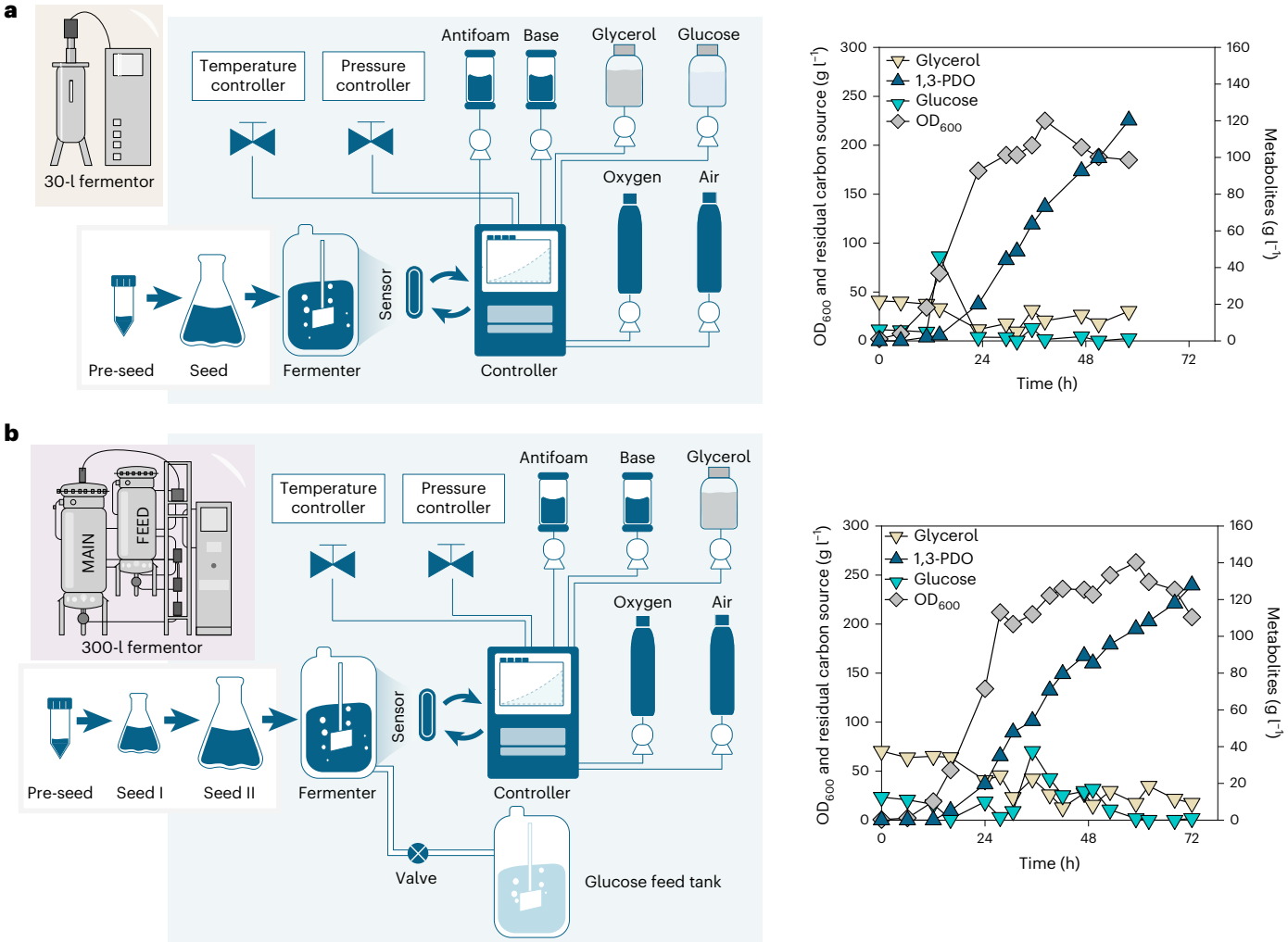

Fig. 6 | Pilot-scale fermentation (30-l and 300-l) demonstration of the PDO2-6 strain harboring plasmids pPCO-aspB and pCS-exp2-panD-sucCD. a, Illustration of a 30-l fermentation system and its fermentation profile. **b**, Illustration of a 300-l fermentation system and its fermentation profile.

1,3-PDO production in flask cultivation, achieving titers of 7.51 g l^{-1} and 7.53 g l^{-1}, both representing approximately a 54% increase compared with the control strain (4.9 g l^{-1}) (Supplementary Fig. 35). We hypothesize that the *sucCD* gene overexpression enhances lower tricarboxylic acid (TCA) cycle flux, improving ATP generation and CoA regeneration, thereby supporting sustained glycerol oxidation and 1,3-PDO formation. In parallel, the *aspA* gene overexpression introduces an additional anaplerotic route toward oxaloacetate, increasing carbon flux through malate and promoting NADPH regeneration via the native malic enzyme pathway. Because YqhD-dependent conversion of 3-HPA to 1,3-PDO requires NADPH, these metabolic effects are consistent with the substantial increases in 1,3-PDO titer observed in both cases.

Fed-batch fermentations were performed in 6.6-l bioreactors to assess the impact of target gene overexpression on 1,3-PDO production at a larger scale. Two strains, each overexpressing a different target gene (*aspA* or *sucCD*), were evaluated (Fig. 4d,e). The strain overexpressing the *aspA* gene (Supplementary Fig. 36, fermentation run 26) showed no improvement over the control strain. By contrast, the strain overexpressing the *sucCD* gene achieved a 1,3-PDO production of 141.5 g l^{-1}, without byproduct accumulation, and outperformed the control strain in both yield (0.61 mol mol^{-1}) and productivity (2.95 g l^{-1} h^{-1}) (Supplementary Fig. 37a, fermentation run 27). This corresponds to a 33% increase in yield and a 43% improvement in productivity compared with the control strain (Supplementary Fig. 33, fermentation run 25). These results demonstrate the efficacy of in silico simulations in identifying effective overexpression targets, leveraging the newly constructed genome-scale metabolic model of *C. glutamicum* SC97. To further assess the industrial relevance of the developed process, we conducted preliminary TEA and LCA based on the current process configuration (Fig. 5 and Supplementary Note 6). For context, the TEA results were compared with reported industrial benchmarks from DuPont, Genencor and Tate & Lyle[39], while the LCA results were compared with data for commercial biobased 1,3-PDO from Primient Covation (formerly DuPont–Tate & Lyle)[40].

Demonstration in 30-l and 300-l pilot-scale fermentation

To assess the scalability of 1,3-PDO production, the final strain overexpressing *sucCD* gene (PDO2-6 harboring pPCO-aspB and pCS-exp2-panD-sucCD) was first subjected to 30-l pilot-scale fermentation without antibiotic supplementation. In 30-l fermentation, 120.2 g l^{-1} of 1,3-PDO was produced, with a productivity and yield of 2.07 g l^{-1} h^{-1} and 0.45 mol mol^{-1} glucose and glycerol, respectively (Fig. 6a). To further evaluate the strain performance on an even larger-scale fermentation, 300-l pilot-scale fermentation was performed using the same strain. The strain produced a 1,3-PDO titer of 127.8 g l^{-1} with a productivity and yield of 1.77 g l^{-1} h^{-1} and 0.33 mol mol^{-1} glucose and glycerol, respectively (Fig. 6b). Although these titers were slightly lower when compared with the titer achieved in 6.6-l laboratory-scale fermentation, this outcome was expected, as the pilot fermentations were conducted

primarily as prototype demonstrations to validate strain robustness and process scalability, rather than fully optimized production runs. Certain limitations were evident at this stage, including reduced yield and productivity probably linked to oxygen transfer and mixing constraints intrinsic to large bioreactor systems. These factors represent engineering aspects to be further improved through optimization of aeration, impeller configuration and feed-control strategies. Such process refinements can be evaluated in conjunction with TEA to quantitatively assess how scale-dependent changes in titer, rate and yield impact overall process economics and energy demand. The absence of antibiotics in both fermentations supports the feasibility of using this strain for commercial production while addressing economic, regulatory and environmental concerns associated with antibiotic use. Despite the scale-up challenges, the strain maintained high titers across scales, demonstrating robust performance under increasingly industrially relevant conditions. These results demonstrate the development of a strain capable of maintaining high production levels in large-scale fermentations.

Discussion

This study presents a comprehensive strategy for the production of 1,3-PDO using *C. glutamicum*, demonstrating its potential as a robust and scalable host for microbial 1,3-PDO biosynthesis. By leveraging advanced systems metabolic engineering, including the construction of a glycerol utilization pathway, the elimination of antibiotic reliance through auxotrophy-based plasmid addiction systems, and in silico simulations to optimize yield and productivity, we achieved high 1,3-PDO titers across scales. The engineered *C. glutamicum* ATCC 13032-derived strain reached a titer of 138 g l^{-1}, while the newly isolated *C. glutamicum* SC97 strain produced 143.9 g l^{-1} in 6.6-l bioreactors. The final production strain, developed without antibiotic supplementation by using an auxotrophy-based plasmid addiction system targeting the *aspB* gene and guided by in silico simulation of the *sucCD* gene overexpression strategy, achieved 1,3-PDO production of 141.5 g l^{-1}. This strain outperformed the control in both yield (0.61 mol mol^{-1}) and productivity (2.95 g l^{-1} h^{-1}). TEA and LCA provided an initial assessment of economic and environmental performance. Upon pilot-scale validation, the same strain produced 127.8 g l^{-1} 1,3-PDO in 300-l fermentation. The demonstrations at larger scales were conducted to confirm strain robustness and scalability under scaled conditions, rather than to represent fully optimized industrial operation. Taken together, these results demonstrate scalable production and provide a basis for subsequent process-level optimization and evaluation. Moreover, the identification of a promoter arising from adaptive laboratory evolution and a native 1,3-PDO exporter provides valuable tools for further metabolic engineering efforts. Further improvement could be achieved through chromosomal integration of the optimized pathway and refinement of large-scale bioprocess parameters, including aeration and feeding strategies, to enhance genetic stability and process performance under industrial conditions. This study demonstrates the effective transition from employing systems metabolic engineering strategies in the model organism (*C. glutamicum* ATCC 13032) to applying and optimizing these strategies in the newly isolated strain (*C. glutamicum* SC97), developed for commercialization purposes. By advancing both strain robustness and process scalability, this work contributes to bridging the gap between laboratory-scale research and subsequent bioprocess optimization.

Methods

Strains and media

All bacterial strains, plasmids and oligonucleotide primers used in this study are listed in Supplementary Tables 4 and 5. *E. coli* DH5α was used for general cloning work. *C. glutamicum* ATCC 13032 was used as a base strain for engineering 1,3-PDO overproduction. For routine work, *E. coli* was grown in Luria–Bertani (LB) broth (10 g l^{-1} of tryptone, 5 g l^{-1} of yeast extract, and 10 g l^{-1} of NaCl) or on LB plates (1.5%, w/v, agar). *C. glutamicum* was routinely grown in BHIS broth (37 g l^{-1} of brain heart infusion and 91 g l^{-1} of sorbitol) or on BHIS plates (1.5%, w/v, agar). When needed, appropriate antibiotics were added: 25 mg l^{-1} of kanamycin (Km) or 100 mg l^{-1} of spectinomycin (Spc) for *E. coli*; 25 mg l^{-1} of Km, 200 mg l^{-1} of Spc and/or 1 mM IPTG for *C. glutamicum*. Details regarding the reagents used in this study are listed in Supplementary Table 26.

Construction of *C. glutamicum* expression plasmids

Construction of all plasmids and Gibson assembly done in this study was performed according to standard procedures[41,42]. Synthesis of all oligonucleotide primers and service of DNA sequencing were provided by Genotech. *E. coli* DH5α strain was used for general cloning work. The *yqhD* gene from *E. coli* with codon optimization to *C. glutamicum* (designated as $yqhD_{opt}$) (Supplementary Table 6) was synthesized at MBIOTECH. Restriction enzymes used in this study were purchased from New England Biolabs. PCR was performed with the C1000 Thermal Cycler (Bio-Rad). The details on plasmid constructions and their primer pairs used for cloning are provided in Supplementary Table 7. All recombinant plasmids were confirmed by colony PCR and DNA sequencing.

Construction of plasmids and strains for genetic manipulation

For CRISPR-based genetic manipulations, the gene-knockout CRISPR plasmids were constructed[32]. In brief, optimal guide RNA targets with the least number of off-targets were designed and synthesized as M9*_F forward primers (Supplementary Table 8) and used with universal reverse primer M5A_R to amplify the single guide RNA (sgRNA) template from pUC19-sgRNA to generate sgRNA fragments. Extension PCR was done with primer pairs M9K_F and M5E_R and individually subcloned to *Stu*I digested pEKts-Cas9 with Gibson assembly to create plasmids pCG9ts-ALD1 to pCG9ts-ALD13. For *sacB*-based genetic manipulations[43], the engineering procedures were performed using a marker-free system employing the *Bacillus subtilis sacB* gene through two rounds of homologous recombination[44]. Cells were transformed by electroporation and plated on BHIS agar containing Km. After incubation at 30 °C for 48 h, colonies were screened for the first recombination by PCR, and the successful ones were subsequently plated on BHIS agar containing 14% (w/v) sucrose for sacB-based counter-selection. Colonies that lost Km resistance were selected, and genomic modifications were confirmed by PCR or sequencing.

Routine *C. glutamicum* transformation protocol

The cells were first grown from glycerol stock in 5 ml BHIS medium for 16 h. Then, 1 ml of cells was inoculated into 50 ml of BHIS medium in an Erlenmeyer flask and cultured for 3–6 h until the OD_{600} reached 1–2. Cells were collected by centrifugation at 4 °C for 5 min at 6,000 rpm (8,054*g*). The cells were then washed with ice-cold sterilized 10% glycerol in distilled water. The cells were then centrifuged and washed one more time. The washed cells were diluted with 500 µl of 10% glycerol. Cells were transformed with about 2 µg DNA by electroporation (1.8 kV and 200–600 Ω), which was immediately followed by adding 700 µl BHIS medium. Then, cells were recovered for 1–2 h at 30 °C, and spread on the BHIS plates containing appropriate antibiotics. Cells were incubated at 30 °C for 2–4 days until colonies appeared. Transformations for genomic manipulations were performed as described above, except that the seed culture was transferred to NCM medium[32] in Erlenmeyer flasks instead of BHIS.

Identification of native aldehyde dehydrogenases using DeepEC

Thirteen proteins were identified as aldehyde dehydrogenases in the *C. glutamicum* strain from the KEGG database. Using a deep-learning-based computational framework DeepEC that predicts EC numbers from protein sequences[31], eight proteins acting as aldehyde dehydrogenase were identified (seven overlapped with those

identified using KEGG database). Gene deletions were performed on 11 of the proteins found in both results. The Python package for DeepEC was installed from the Bitbucket repository, and the protein FASTA file, which was used as input for DeepEC, was downloaded from GenBank (GCA_000011325.1).

Genome manipulation using CRISPR–Cas9-assisted recombineering for native aldehyde dehydrogenase screening

The deletion of each target gene in *C. glutamicum* ATCC 13032 was done using CRISPR–Cas9-assisted recombineering method[32]. To summarize the procedure, competent cells of *C. glutamicum* ATCC 13032 harboring pTacCC1-HrT were transformed by electroporation with pCG9ts-ALD1 and ssODN_ALD1 (Supplementary Table 9) to yield the WAH1 strain. Deletion for the other 12 targets was done similarly, with the respective pCG9 plasmid/ssODN pairs. To screen the strain with the least 3-HP accumulation, flask cultivation of the 13 engineered strains harboring pCS-glpFKD and pEK-pdu-yE was done using modified CGXII media. After 48 h of culture, the supernatant was analyzed through high-performance liquid chromatography to compare 3-HP accumulation in each strain.

1,3-PDO toxicity test

1,3-PDO toxicity to the wild-type *C. glutamicum* ATCC 13032, *E. coli* W3110 and *K. pneumoniae* KCTC 2952 was investigated in shake-flask cultures. Pre-seed culture of the *C. glutamicum* strain was cultured for 16 h at 200 rpm and 30 °C in a 50-ml conical tube containing 5 ml of BHIS. For *E. coli* and *K. pneumoniae*, both strains were cultured for 12 h at 200 rpm and 37 °C in 25-ml test tubes containing 10 ml LB medium. Then, cells were inoculated to 300-ml baffled flasks containing 25 ml CGXII medium with 40 g l^{-1} glucose as the sole carbon source for *C. glutamicum*, and to 50 ml MR medium. The MR medium (pH 6.8) contains (per liter) 4 g $(NH_4)_2HPO_4$, 6.67 g KH_2PO_4, 0.8 g citric acid, 0.8 g $MgSO_4{\cdot}7H_2O$ and 5 ml of a trace metal solution (10 g $FeSO_4{\cdot}7H_2O$, 2.2 g $ZnSO_4{\cdot}7H_2O$, 1 g $CuSO_4{\cdot}5H_2O$, 0.58 g $MnSO_4{\cdot}5H_2O$, 0.02 g $Na_2B_4O_7{\cdot}10H_2O$, 2 g $CaCl_2{\cdot}2H_2O$ and 0.1 g $(NH_4)_6Mo_7O_{24}$ per liter of 5 M HCl). The cells were transferred to match the starting OD_{600} of 0.2 for *C. glutamicum* and 0.05 for *E. coli* and *K. pneumoniae*. The 1,3-PDO stock solution was added to the flask at the beginning in different concentrations indicated. Control flasks without 1,3-PDO addition were also cultured. Flasks were cultured for 24 h at 200 rpm at 30 °C for *C. glutamicum* and 37 °C for *E. coli* and *K. pneumoniae*. Cell growth was monitored by measuring OD_{600}.

Abridged-Adaptive Laboratory Evolution (Ab-ALE)

C. glutamicum W13G strain was grown in 25 ml CGXII medium[28] in 300-ml baffled flasks. Initial glycerol concentration was set to 10 g l^{-1}, 20 g l^{-1} and 40 g l^{-1}, and the shake-flask cultivation was done in triplicates. After 48 h, one of the strains grown in 20 g l^{-1} glycerol grew the fastest among all the other glycerol conditions. The fastest-growing strain was chosen for Ab-ALE, where ALE was done over eight generations, transferring 250 µl of inoculum from the previous flask to the next flask containing 25 ml of fresh media. The fifth to eighth generation was done with an initial glycerol concentration of 40 g l^{-1} as opposed to 20 g l^{-1} as in earlier generations.

Cultivation conditions

Flask cultivations of *C. glutamicum* were conducted in 300-ml baffled flasks containing 25 ml of modified CGXII medium (Supplementary Table 10) supplemented with 40 g l^{-1} of carbon source. The carbon source composition used is as mentioned in each cultivation. Both seed and flask cultures were done at 200 rpm and 30 °C. The seed culture was inoculated from the glycerol stock in 5 ml BHIS medium for 16 h. The seed was transferred to the flask medium to match the starting OD_{600} of 0.1 and cultured for 48 h. Cells were induced by adding 1 mM IPTG from the beginning of the culture unless otherwise mentioned.

Fed-batch fermentations were performed in a 6.6-l jar fermenter (Bioflo 320; New Brunswick Scientific) containing 1.8 l modified CGXII medium (Supplementary Table 10). Cells were spread onto BHIS agar plates and then incubated at 30 °C for 24 h. Then, the pre-seed culture was prepared by inoculating the cells from the plate to a 50-ml conical tube containing 5 ml of BHIS medium. Both pre-seed and seed cultures were incubated at 200 rpm and 30 °C. After 16 h, the pre-seed culture was transferred into four 50-ml seed cultures in 300-ml baffled flasks, and the volume of cells transferred was adjusted to achieve an initial OD_{600} of 0.1. After 24 h, 200 ml of the seed culture was transferred to the fermenter. For microaerobic fermentations, the agitation was maintained at 600 rpm and the air flow rate was maintained at 0.5 l min^{-1}. For aerobic fermentations, the air flow rate was maintained at 2 l min^{-1}, dissolved oxygen levels were maintained at 10% with agitation ranging from 600 rpm to 1,000 rpm, and pure oxygen was injected after reaching maximum agitation. For manual feeding conditions, feeding solution was manually added each time the residual substrate level decreased to <10 g l^{-1}. For pH-stat feeding, the feeding was added whenever pH rose above 7.20 for glucose and whenever pH rose above 7.05 for glycerol only fermentations. For all fed-batch fermentations including the pilot-scale fermentation, the pH was maintained at 7.0 by the addition of 28% (v/v) NH_4OH solution (Junsei Chemical) and the temperature was maintained at 30 °C. Foaming was suppressed by adding antifoam 204 (Sigma-Aldrich). The feeding solution composition is provided in Supplementary Table 11.

The pilot-scale fermentations were performed using 30-l and 300-l fermenters (KoBioTech) containing modified CGXII medium (9 l for 30-l fermentation, and 90 l for 300-l fermentation) (Supplementary Table 12). For both fermentations, the pre-seed culture was prepared by inoculating the cells from the plate into a 50-ml conical tube containing 5 ml BHIS medium. All pre-seed and seed cultures were grown at 30 °C in a shaking incubator (200 rpm). For 30-l fermentation, after 16 h, the pre-seed culture was transferred to two 2-l baffled flasks containing 500 ml seed medium, and the starting culture OD_{600} was matched to 0.1. After 24 h, the seed culture was transferred to the 30-l fermenter. For 300-l fermentation, after 16 h, the pre-seed culture was transferred to two 300-ml baffled flasks containing 50 ml of the seed medium, and the starting culture OD_{600} was matched to 0.1. After 16 h, the seed culture was transferred to five 3-l baffled flasks, each containing 1 l seed medium. Similarly, the cells were transferred to match the seed culture to OD_{600} 0.1. After 24 h, the seed culture was transferred to the 300-l fermenter. For both fermentations, the dissolved oxygen levels were maintained at 10%, with agitation ranging from 150 rpm to 450 rpm for 30 l and 100 to 350 rpm for 300 l, and pure oxygen was injected after reaching maximum agitation. For both fermentations, the glycerol was supplemented manually. The glucose feeding was performed by using the pH-stat feeding, and added whenever pH rose above 7.1. For all fed-batch fermentations reported in this study, excess glycerol was intentionally maintained during manual feeding to avoid substrate limitation. Residual glycerol concentrations in the broth were fully subtracted from the total glycerol fed, and all reported yields were calculated based solely on the consumed substrate. Product titer was calculated based on concentrations measured in the fermentation supernatant, whereas yield was calculated as the total amount of product formed relative to the total substrate consumed, without correction for biomass volume. For interested readers, biomass volume-adjusted yields are provided in Supplementary Table 1.

Serial-transfer flask cultivation

Serial-transfer flask cultivation was performed using the final production strain (PDO2-6 harboring pPCO-aspB and pCS-exp2-panD-sucCD). Flask cultivation was conducted under the same conditions described in the general cultivation section, using CGXII medium supplemented with 40 g l^{-1} of glycerol and 40 g l^{-1} of glucose. For each transfer cycle, cultures were inoculated to an initial OD_{600} of 0.2 in 25 ml working

volume per flask. At the end of each cycle, OD_{600} and 1,3-PDO concentrations were measured, and the culture was transferred into fresh medium to initiate the next cycle.

Genomic DNA extraction and qPCR analysis

For genomic DNA extraction, cells collected at 24 h and 96 h of the serial-transfer flask cultivation experiment were normalized to an OD_{600} of 3 in a 1 ml volume. The genomic DNA was extracted from the cells by AccuPrep Genomic DNA Extraction Kit (Bioneer), and the qPCR was performed using AccuPower GreenStar qPCR PreMix (Bioneer), following the manufacturer's instructions. The qPCR was performed using QuantStudio Real-Time PCR System (Applied Biosystems, Waltham). For the chromosomal reference, primers NCgl2772_F/NCgl2772_R were used[45]. For the pPCO-aspB and pCS-exp2-panD-sucCD retention evaluation, the primer pairs pdu_F/pdu_R and exp_F/exp_R were used, respectively.

Analytical methods

Cell growth was monitored by measuring optical density at 600 nm (OD_{600}) with an Ultrospec 3000 spectrophotometer (Amersham Biosciences). The concentration of metabolites such as glucose, glycerol, 1,3-PDO, lactate and others was analyzed using a Waters 1515 high-performance liquid chromatograph (Waters) equipped with Waters 2414 refractive index detectors. The 3-HP concentration was measured using high-performance liquid chromatography (Agilent 1100 series with diode array detector (DAD) detectors and an Agilent MetaCarb 87H column, with detection at 210 nm) using 0.1% H_3PO_4 at 40 °C at a flow rate of 0.5 ml min^{-1}.

In silico simulation

Simulations to identify downregulation targets for increasing the NADPH pool for 1,3-PDO production were conducted using the Flux Variability Scanning based on Enforced Objective Flux (FVSEOF) algorithm. The FVSEOF algorithm systematically enforces flux through reactions while performing flux variability analysis to identify key targets that can enhance the production of desired metabolites[46]. An artificial NADPH external equation was incorporated into the metabolic model and set as the objective function to identify downregulation target genes using the FVSEOF algorithm.

Next, additional simulations were conducted to identify the overexpression targets to enhance 1,3-PDO production. The simulation was carried out as follows. First, flux balance analysis was performed to determine the minimum and maximum flux values for 1,3-PDO production. Next, the range between the minimum and maximum values was evenly divided, and constraint conditions were applied incrementally from the minimum to the maximum value. For each constraint on 1,3-PDO, the cell growth rate was maximized to obtain the maximum growth rate under the given condition. Then, the reference flux was calculated by maximizing the cell growth rate. Finally, the least absolute deviation regression was used to minimize the difference between the reference flux and the constraints on 1,3-PDO production and cell growth values determined in the previous steps[47]. Through statistical analysis of the resulting intracellular flux distributions, reactions exhibiting a linear positive correlation with the 1,3-PDO production rate were designated as overexpression targets.

TEA and LCA

Process simulations were carried out in Aspen Plus (version 15, Aspen Technology) under steady-state conditions, and economic evaluation was conducted using the Aspen Process Economic Analyzer (APEA). The process was divided into modules for medium preparation, seed train, fermentation, recovery, purification and utilities reflecting the configuration set by the Hanwha Solutions facility. Installed equipment costs (inside battery limits, ISBL) were estimated using the Bare Module Cost method[48], in which base purchase costs are scaled to equipment capacity using a six-tenths rule and corrected for construction material and operating pressure. The ISBL cost was calculated as 73.24 billion KRW (US$52.31 million). The currency exchange rate used in this analysis was assumed to be US$1 = 1,400 KRW. The outside battery limits cost, including utilities, wastewater treatment and supporting infrastructure, was assumed to be 50% of ISBL, resulting in a total installed capital investment of 109.86 billion KRW (US$78.47 million). The design basis assumed a working fermenter volume of 300 m^3 operated in 48-h fed-batch mode followed by 12 h for preparation and turnaround, giving 60 h per batch and 133 batches per year. Under these conditions, the annual 1,3-PDO production capacity is 5,600 metric tons (Supplementary Table 19). Operating costs were calculated from simulated consumption of glucose, glycerol, vitamin B_{12}, steam, electricity and cooling water using current Korean industrial prices and converted to US dollars using the same exchange rate (Supplementary Tables 20–22). A plant lifetime of 15 years and straight-line depreciation were assumed. Net operating profit less adjusted taxes, free cash flow and internal rate of return (IRR) were evaluated using discounted cash-flow analysis based on a 15-year project lifetime. Sensitivity analysis was conducted by varying the 1,3-PDO selling price and key raw-material prices (Supplementary Tables 20 and 23). Detailed stream conditions for each stage of the process flowsheet are provided in Supplementary Table 22.

LCA was conducted using material-balance data obtained from the Aspen Plus simulation (Supplementary Tables 19 and 24). The system boundary was defined as cradle-to-gate and included feedstock production and biochemical conversion, while excluding utilities (steam, electricity and cooling water), wastewater treatment and infrastructure. The functional unit was 1 kg of 1,3-PDO, and climate change potential (kg CO_2 equivalents per kg of 1,3-PDO) was used as the primary environmental indicator. Greenhouse gas emissions were quantified using carbon-footprint values for glucose and glycerol obtained from OpenLCA datasets (Supplementary Table 24). Biogenic CO_2 uptake, land-use-change impacts and energy credits were not considered. Feedstock consumption values were extracted from the fermentation stoichiometry in the model, corresponding to 1.13 kg glucose and 0.76 kg glycerol required per kilogram of 1,3-PDO produced, or 1.26 and 0.85 kg per kg final product assuming 90% downstream recovery (Supplementary Table 24a). Total climate-change impact was calculated as the sum of feedstock-specific contributions.

Genome sequencing and analysis

Whole bacterial genome sequencing was performed by Plasmidsaurus using Oxford Nanopore Technology with custom analysis and annotation. Reads were aligned to the parental *C. glutamicum* ATCC 13032 reference genome (GenBank accession number NC_003450.3), and mutations were predicted using Breseq v0.39.0 computational pipeline[49]. A presence–absence matrix of mutations present in each clone was then generated (Supplementary Table 25). The parental strain W13G has 29 mutations relative to the *C. glutamicum* ATCC 13032 reference genome. GenomeDiff files for W13G and the evolved strain W13g were analyzed using the gdtools COMPARE function in Breseq to compile all detected variants. Mutations were then parsed to identify those uniquely present in W13g, which represent evolution-associated genetic changes potentially contributing to the improved 1,3-PDO phenotype.

Reporting summary

Further information on research design is available in the Nature Portfolio Reporting Summary linked to this article.

Data availability

All datasets analyzed during the current study are presented in this Article and its Supplementary Information. Source data are provided with this paper. These data are also available via Figshare at https://doi.org/10.6084/m9.figshare.29264624 (ref. 50). The genome sequencing data for *Corynebacterium glutamicum* SC97 have been deposited in

the NCBI under accession number JBSORY000000000 (BioProject PRJNA1370509). Process simulations were carried out in Aspen Plus (version 15, Aspen Technology).

Code availability

The computational pipeline for constructing the resources is available via GitHub at https://github.com/kaistsystemsbiology/SC97-GEM.

References

1. Lee, S. Y. et al. Author Correction: a comprehensive metabolic map for production of bio-based chemicals. *Nat. Catal.* **2**, 942–944 (2019).
2. Borugadda, V. B. & Goud, V. V. Biodiesel production from renewable feedstocks: status and opportunities. *Renew. Sustain. Energy Rev.* **16**, 4763–4784 (2012).
3. Salvi, B. L. & Panwar, N. L. Biodiesel resources and production technologies – a review. *Renew. Sustain. Energy Rev.* **16**, 3680–3689 (2012).
4. Brahma, S. et al. Biodiesel production from mixed oils: a sustainable approach towards industrial biofuel production. *Chem. Eng. J. Adv.* **10**, 100284 (2022).
5. Yang, F., Hanna, M. A. & Sun, R. Value-added uses for crude glycerol—a byproduct of biodiesel production. *Biotechnol. Biofuels* **5**, 13 (2012).
6. Pagliaro, M., Ciriminna, R., Kimura, H., Rossi, M. & Della Pina, C. From glycerol to value-added products. *Angew. Chem. Int. Ed.* **46**, 4434–4440 (2007).
7. Lima, P. J. M. et al. An overview on the conversion of glycerol to value-added industrial products via chemical and biochemical routes. *Biotechnol. Appl. Biochem.* **69**, 2794–2818 (2022).
8. Anitha, M., Kamarudin, S. K. & Kofli, N. T. The potential of glycerol as a value-added commodity. *Chem. Eng. J.* **295**, 119–130 (2016).
9. Niaounakis, M. in *Biopolymers: Processing and Products* (ed. M. Niaounakis) 79–116 (William Andrew Publishing, 2015).
10. Gallezot, P. Catalytic routes from renewables to fine chemicals. *Catal. Today* **121**, 76–91 (2007).
11. Lee, S. Y. & Kim, H. U. Systems strategies for developing industrial microbial strains. *Nat. Biotechnol.* **33**, 1061–1072 (2015).
12. Soucaille, P. Process for the biological production of 1,3-propanediol from glycerol with high yield. US patent US8236994B2 (2012).
13. Choi, K. R. et al. Systems metabolic engineering strategies: integrating systems and synthetic biology with metabolic engineering. *Trends Biotechnol.* **37**, 817–837 (2019).
14. Nakamura, C. E. & Whited, G. M. Metabolic engineering for the microbial production of 1,3-propanediol. *Curr. Opin. Biotechnol.* **14**, 454–459 (2003).
15. Zhu, F., Liu, D. & Chen, Z. Recent advances in biological production of 1,3-propanediol: new routes and engineering strategies. *Green Chem.* **24**, 1390–1403 (2022).
16. Celinska, E. Debottlenecking the 1,3-propanediol pathway by metabolic engineering. *Biotechnol. Adv.* **28**, 519–530 (2010).
17. Fokum, E., Zabed, H. M., Yun, J., Zhang, G. & Qi, X. Recent technological and strategical developments in the biomanufacturing of 1,3-propanediol from glycerol. *Int. J. Environ. Sci. Technol.* **18**, 2467–2490 (2021).
18. da Silva Ruy, A. D. et al. Catalysts for glycerol hydrogenolysis to 1,3-propanediol: a review of chemical routes and market. *Catal. Today* **381**, 243–253 (2021).
19. Zhu, Y. et al. Current advances in microbial production of 1,3-propanediol. *Biofuels Bioprod. Biorefining* **15**, 1566–1583 (2021).
20. Inui, M. & Toyoda, K. *Corynebacterium glutamicum*: *Biology and Biotechnology* (Springer, 2020).
21. Wendisch, V. F. Metabolic engineering advances and prospects for amino acid production. *Metab. Eng.* **58**, 17–34 (2020).
22. Chai, M. et al. Synthetic biology toolkits and metabolic engineering applied in *Corynebacterium glutamicum* for biomanufacturing. *ACS Synth. Biol.* **10**, 3237–3250 (2021).
23. Becker, J., Rohles, C. M. & Wittmann, C. Metabolically engineered *Corynebacterium glutamicum* for bio-based production of chemicals, fuels, materials, and healthcare products. *Metab. Eng.* **50**, 122–141 (2018).
24. Li, Z. et al. Systems metabolic engineering of *Corynebacterium glutamicum* for high-level production of 1,3-propanediol from glucose and xylose. *Metab. Eng.* **70**, 79–88 (2022).
25. Huang, J. et al. Cofactor recycling for co-production of 1,3-propanediol and glutamate by metabolically engineered *Corynebacterium glutamicum*. *Sci. Rep.* **7**, 42246 (2017).
26. Rittmann, D., Lindner, S. N. & Wendisch, V. F. Engineering of a glycerol utilization pathway for amino acid production by *Corynebacterium glutamicum*. *Appl. Environ. Microbiol.* **74**, 6216–6222 (2008).
27. Wang, C., Cai, H., Chen, Z. & Zhou, Z. Engineering a glycerol utilization pathway in *Corynebacterium glutamicum* for succinate production under O2 deprivation. *Biotechnol. Lett.* **38**, 1791–1797 (2016).
28. Eggeling, L. & Bott, M. *Handbook of Corynebacterium glutamicum* (Taylor & Francis, 2005).
29. Chen, Z. et al. Metabolic engineering of *Corynebacterium glutamicum* for the production of 3-hydroxypropionic acid from glucose and xylose. *Metab. Eng.* **39**, 151–158 (2017).
30. Chang, Z. et al. Enhanced 3-hydroxypropionic acid production from acetate via the malonyl-CoA pathway in *Corynebacterium glutamicum*. *Front. Bioeng. Biotechnol.* **9**, 808258 (2022).
31. Ryu, J. Y., Kim, H. U. & Lee, S. Y. Deep learning enables high-quality and high-throughput prediction of enzyme commission numbers. *Proc. Natl Acad. Sci. USA* **116**, 13996–14001 (2019).
32. Cho, J. S. et al. CRISPR/Cas9-coupled recombineering for metabolic engineering of *Corynebacterium glutamicum*. *Metab. Eng.* **42**, 157–167 (2017).
33. Kim, S. Y., Lee, J. & Lee, S. Y. Metabolic engineering of *Corynebacterium glutamicum* for the production of L-ornithine. *Biotechnol. Bioeng.* **112**, 416–421 (2015).
34. Park, S. H. et al. Metabolic engineering of *Corynebacterium glutamicum* for L-arginine production. *Nat. Commun.* 5, 4618 (2014).
35. Tsuge, Y. & Yamaguchi, A. Physiological characteristics of *Corynebacterium glutamicum* as a cell factory under anaerobic conditions. *Appl. Microbiol. Biotechnol.* **105**, 6173–6181 (2021).
36. Zhang, Y., Dong, R., Zhang, M. & Gao, H. Native efflux pumps of *Escherichia coli* responsible for short and medium chain alcohol. *Biochem. Eng. J.* **133**, 149–156 (2018).
37. Dusch, N., Pühler, A. & Kalinowski, J. Expression of the *Corynebacterium glutamicum panD* gene encoding l-aspartate-α-decarboxylase leads to pantothenate overproduction in *Escherichia coli*. *Appl. Environ. Microbiol.* **65**, 1530–1539 (1999).
38. Machado, D., Andrejev, S., Tramontano, M. & Patil, K. R. Fast automated reconstruction of genome-scale metabolic models for microbial species and communities. *Nucleic Acids Res.* **46**, 7542–7553 (2018).
39. *1,3-Propanediol (PDO) via Aerobic Fermentation of Glucose* Yearbook 2013, Report 1M-1169 (IHS Chemical Process Economics Program, 2013).
40. Primient Covation LLC. *Life Cycle Impact Assessment (LCIA) Results for Susterra® and Zemea® 1,3-Propanediol (Bio-PDO™). Technical case study (2023).* (SpecialChem, accessed 28 November 2025); https://www.specialchem.com/media/documents/pdf/primient-covation-biopdo-lca-letter.pdf

41. Sambrook, J. & Russell, D. W. *Molecular Cloning: A Laboratory Manual* 3rd edn (Cold Spring Harbor Laboratory Press, 2001).
42. Gibson, D. G. et al. Enzymatic assembly of DNA molecules up to several hundred kilobases. *Nat. Methods* **6**, 343–345 (2009).
43. Schafer, A. et al. Small mobilizable multi-purpose cloning vectors derived from the *Escherichia coli* plasmids pK18 and pK19: selection of defined deletions in the chromosome of *Corynebacterium glutamicum*. *Gene* **145**, 69–73 (1994).
44. Cho, J. S. et al. Targeted and high-throughput gene knockdown in diverse bacteria using synthetic sRNAs. *Nat. Commun.* **14**, 2359 (2023).
45. Wang, X. et al. Identification and validation of appropriate reference genes for qRT–PCR analysis in *Corynebacterium glutamicum*. *FEMS Microbiol. Lett.* **365**, fny030 (2018).
46. Park, J. M. et al. Flux variability scanning based on enforced objective flux for identifying gene amplification targets. *BMC Syst. Biol.* **6**, 1–11 (2012).
47. Kim, W. J. et al. Genome-wide identification of overexpression and downregulation gene targets based on the sum of covariances of the outgoing reaction fluxes. *Cell Syst.* **14**, 990–1001 (2023).
48. Seider, W. D., Seader, J. D., Lewin, D. R. & Widagdo, S. *Product and Design Principles: Synthesis, Analysis, and Evaluation* 3rd edn (John Wiley & Sons, 2010).
49. Deatherage, D. E. & Barrick, J. E. Identification of mutations in laboratory-evolved microbes from next-generation sequencing data using breseq. *Methods Mol. Biol.* **1151**, 165–188 (2014).
50. Cho, J.S., Prabowo, C.P.S., Han, T., Moon, C.W., Ko, Y-S., Cho, C. et al. High-titer, antibiotic-free, pilot-scale production of 1,3-propanediol by engineered *Corynebacterium*. Data. *figshare* https://doi.org/10.6084/m9.figshare.29264624 (2026).

Acknowledgements

We thank K. J. Jeong for generously providing us with *C. glutamicum* strain WT bioD::sfGFP for this study. This work was supported by Hanwha Solutions through the KAIST-Hanwha Solutions Future Technology Institute. Development of systems metabolic engineering tools was supported by the Development of Platform Technologies of Microbial Cell Factories for Next-Generation Biorefineries project (2022M3J5A1056117), funded by the National Research Foundation of Korea and supported by the Korean Ministry of Science and ICT.

Author contributions

S.Y.L. conceived the project. J.S.C., C.P.S.P. and S.Y.L. conceptualized the project. J.S.C. and C.P.S.P. designed the experiments. J.S.C., C.P.S.P., T.H., C.W.M., Y.-S.K., C.C., J.W.K., W.J.K., H.B.B., J.E.L., M.K. and N.J. performed the experiments. J.S.C., C.P.S.P., T.H., C.W.M., Y.-S.K., C.C., J.W.K., W.J.K. and H.B.B. analyzed the data. J.S.C. and C.P.S.P. wrote the paper. J.S.C., C.P.S.P. and S.Y.L. reviewed and edited the paper. All authors read and approved the final paper.

Competing interests

S.Y.L., J.S.C., C.P.S.P., T.H., C.W.M., Y.-S.K., C.C., J.W.K., W.J.K. and H.B.B. declare that the strains developed here are of commercial interest and have filed patents. S.Y.L., J.S.C., J.W.K., Y.-S.K., C.P.S.P. and T.H. have filed patent application numbers KR 10-2018-0005451, PCT/KR2019/000571, US 16962213, JP 2020-540381, EP 19740842.0 and CN 201980016833.8, patent registration numbers KR 10-2103408-0000 and JP 7129484, covering the microorganism capable of producing 1,3-PDO from glycerol as a sole carbon source by introducing a 1,3-PDO biosynthetic pathway into the strain. S.Y.L., J.S.C., J.W.K., Y.-S.K., C.P.S.P. and T.H. have filed patent application numbers KR 10-2018-0058952, PCT/KR2019/004961, US 17055971, JP 2020-565891, EP 19808016.0 and CN 201980044658.3, patent registration numbers KR 10-2201720-0000, US 11473111, JP 7046229 and ZL201980044658.3, covering a mutant *Corynebacterium glutamicum* strain in which 3-HP production is suppressed, thereby enabling efficient production of 1,3-PDO. S.Y.L., J.S.C., T.H., C.P.S.P. and C.C. have filed patent application number KR 10-2024-0087809, covering a novel synthetic promoter in the *Corynebacterium* genus. S.Y.L., H.B.B., W.J.K., C.C., C.P.S.P., Y.-S.K., T.H. and C.W.M. have filed patent application number KR 10-2023-0093445, covering the novel 1,3-PDO exporter protein and the microorganism capable of producing 1,3-PDO with the novel 1,3-PDO exporter. S.Y.L., H.B.B., W.J.K., C.C., C.P.S.P., T.H. and C.W.M. have filed patent application number KR 10-2024-0198710, covering microbial engineering strategies related to 1,3-PDO biosynthesis described in this study. C.C., W.J.K. and H.B.B. are employees of Hanwha Solutions Company. The other authors declare no competing interests.

Additional information

Supplementary information The online version contains supplementary material available at https://doi.org/10.1038/s44286-026-00389-w.

Correspondence and requests for materials should be addressed to Sang Yup Lee.

Peer review information *Nature Chemical Engineering* thanks Zhen Chen, Shihui Yang and the other, anonymous, reviewer(s) for their contribution to the peer review of this work. Peer reviewer reports are available.

nature portfolio

Corresponding author(s): Sang Yup Lee

Last updated by author(s): Mar 21, 2026

Reporting Summary

Nature Portfolio wishes to improve the reproducibility of the work that we publish. This form provides structure for consistency and transparency in reporting. For further information on Nature Portfolio policies, see our Editorial Policies and the Editorial Policy Checklist.

Statistics

For all statistical analyses, confirm that the following items are present in the figure legend, table legend, main text, or Methods section.

n/a	Confirmed
☐	☒ The exact sample size (*n*) for each experimental group/condition, given as a discrete number and unit of measurement
☒	☐ A statement on whether measurements were taken from distinct samples or whether the same sample was measured repeatedly
☒	☐ The statistical test(s) used AND whether they are one- or two-sided *Only common tests should be described solely by name; describe more complex techniques in the Methods section.*
☒	☐ A description of all covariates tested
☒	☐ A description of any assumptions or corrections, such as tests of normality and adjustment for multiple comparisons
☐	☒ A full description of the statistical parameters including central tendency (e.g. means) or other basic estimates (e.g. regression coefficient) AND variation (e.g. standard deviation) or associated estimates of uncertainty (e.g. confidence intervals)
☒	☐ For null hypothesis testing, the test statistic (e.g. *F*, *t*, *r*) with confidence intervals, effect sizes, degrees of freedom and *P* value noted *Give P values as exact values whenever suitable.*
☒	☐ For Bayesian analysis, information on the choice of priors and Markov chain Monte Carlo settings
☒	☐ For hierarchical and complex designs, identification of the appropriate level for tests and full reporting of outcomes
☒	☐ Estimates of effect sizes (e.g. Cohen's *d*, Pearson's *r*), indicating how they were calculated

Our web collection on statistics for biologists contains articles on many of the points above.

Software and code

Policy information about availability of computer code

Data collection	OpenLAB CDS(ChemStation C.01.07 SR4 Edition) and Breeze2(Database version 6.20.00.00) were used for collecting metabolite concentrations in shake-flask and fed-batch fermentation samples. Custom code used for constructing the resources is available at https://github.com/kaistsystemsbiology/SC97-GEM. The genome sequencing data for Corynebacterium glutamicum SC97 have been deposited in the NCBI BioProject database under accession number PRJNA1370509. Process simulations were carried out in Aspen Plus® (Version 15, Aspen Technology Inc.)
Data analysis	OpenLAB CDS(ChemStation C.01.07 SR4 Edition) and Breeze2(Database version 6.20.00.00) were used for collecting metabolite concentrations in shake-flask and fed-batch fermentation samples. Custom code used for constructing the resources is available at https://github.com/kaistsystemsbiology/SC97-GEM. The genome sequencing data for Corynebacterium glutamicum SC97 have been deposited in the NCBI BioProject database under accession number PRJNA1370509. Process simulations were carried out in Aspen Plus® (Version 15, Aspen Technology Inc.)

For manuscripts utilizing custom algorithms or software that are central to the research but not yet described in published literature, software must be made available to editors and reviewers. We strongly encourage code deposition in a community repository (e.g. GitHub). See the Nature Portfolio guidelines for submitting code & software for further information.

Data

Policy information about availability of data

All manuscripts must include a data availability statement. This statement should provide the following information, where applicable:

- Accession codes, unique identifiers, or web links for publicly available datasets
- A description of any restrictions on data availability
- For clinical datasets or third party data, please ensure that the statement adheres to our policy

All datasets analyzed during the current study are presented in this manuscript, the Supplementary Information, and Source Data are provided with this paper and also available from Figshare: https://doi.org/10.6084/m9.figshare.29264624. The genome sequencing data for Corynebacterium glutamicum SC97 have been deposited in the NCBI BioProject database under accession number PRJNA1370509. Process simulations were carried out in Aspen Plus® (Version 15, Aspen Technology Inc.)

Research involving human participants, their data, or biological material

Policy information about studies with human participants or human data. See also policy information about sex, gender (identity/presentation), and sexual orientation and race, ethnicity and racism.

Reporting on sex and gender	Not applicable to this study
Reporting on race, ethnicity, or other socially relevant groupings	Not applicable to this study
Population characteristics	Not applicable to this study
Recruitment	Not applicable to this study
Ethics oversight	Not applicable to this study

Note that full information on the approval of the study protocol must also be provided in the manuscript.

Field-specific reporting

Please select the one below that is the best fit for your research. If you are not sure, read the appropriate sections before making your selection.

☒ Life sciences ☐ Behavioural & social sciences ☐ Ecological, evolutionary & environmental sciences

For a reference copy of the document with all sections, see nature.com/documents/nr-reporting-summary-flat.pdf

Life sciences study design

All studies must disclose on these points even when the disclosure is negative.

Sample size	Shake-flask experiments were done in triplicates, which is a normally employed sample size to ensure biological reproducibility, unless otherwise specified. 6.6-l fed-batch fermentations of the final engineered strain was repeated for reproducibility due to their limited availability.
Data exclusions	No data were excluded from the analyses.
Replication	Shake-flask experiments were done in triplicates, which is a normally employed sample size to ensure biological reproducibility, unless otherwise specified. 6.6-l fed-batch fermentations of the final engineered strain was repeated for reproducibility due to their limited availability.
Randomization	Single colonies were randomly selected from plates and randomly allocated into experimental groups, each of which was subjected to independent flask cultures and analyses.
Blinding	The researchers were blinded to the group allocation by randomly selecting single colonies multiple times.

Reporting for specific materials, systems and methods

We require information from authors about some types of materials, experimental systems and methods used in many studies. Here, indicate whether each material, system or method listed is relevant to your study. If you are not sure if a list item applies to your research, read the appropriate section before selecting a response.

Materials & experimental systems

n/a	Involved in the study
☒	☐ Antibodies
☒	☐ Eukaryotic cell lines
☒	☐ Palaeontology and archaeology
☒	☐ Animals and other organisms
☒	☐ Clinical data
☒	☐ Dual use research of concern
☒	☐ Plants

Methods

n/a	Involved in the study
☒	☐ ChIP-seq
☒	☐ Flow cytometry
☒	☐ MRI-based neuroimaging

Plants

Seed stocks	Not applicable to this study
Novel plant genotypes	Not applicable to this study
Authentication	Not applicable to this study